Microchimica Acta (2021) 188: 26
https://doi.org/10.1007/s00604-020-04667-z

ORIGINAL PAPER

Gold nanocluster-europium(III) ratiometric fluorescence assay for dipicolinic acid

Xiaoqing Li[1] · Junjun Luo[1] · Xingxing Jiang[1] · Minghui Yang[1] · Avraham Rasooly[2]

Received: 5 May 2020 / Accepted: 23 November 2020 / Published online: 6 January 2021

Abstract

A ratiometric fluorescence assay was designed for determination of dipicolinic acid (DPA), a spore-specific compound which is used as a biomarker for *Bacillus anthracis* spores for food and medical product safety analysis. The dual-channel fluorescence probe integrates two fluorescent materials, Eu^{3+} ion and gold nanocluster (Au NC). The Au NC is used as a reference channel to measure background noise and the Eu^{3+} ion as the DPA-specific response signal channel. The probe was prepared through simply combing bovine serum albumin (BSA)-scaffolded Eu^{3+} ion and Au NCs. When excited at 530 nm, in the presence of DPA, the fluorescence signals of Eu^{3+} ion at 595, 617, and 695 nm increased significantly while the 650 nm signal of Au NC reference remained relatively constant. This fluorescence probe has good photo-stability and also displays good selectivity and high sensitivity for DPA with a low detection limit of 0.8 μM. The linear range of the ratiometric probe for DPA is 1–50 μM. For determination of DPA released during the germination of *Bacillus subtilis* spores, the detection results were in agreement with measurements by conventional calorimetry assay. The method may have potential for measuring the level of contamination and germination by spores.

Keywords Fluorescence detection · Dipicolinic acid · Gold nanocluster · Ratiometric fluorescence · *Bacillus subtilis*

Introduction

For fluorescence detection, especially for the widely used single-signal fluorescence probes, the detection is often affected by sample background noise [1–3]. Ratiometric fluorescent probe, which uses the intensity ratio of two fluorescence peaks at different wavelengths as signal and reference channel, can provide a built-in correction of the background interference, leading to improved signal to noise ratio measurement, and better detection sensitivity and accuracy [4–6].

The basic requirement for ratiometric fluorescence detection is to synthesize fluorescent probes with at least two emission wavelengths. The traditional probe materials include organic dyes, fluorescent nanomaterials, and lanthanide ions [7–9]. Metal nanoclusters, such as gold nanoclusters (Au NCs), are a new type of luminescent nanomaterial that is often used for the detection of heavy metal ions [10], inorganic anions [11], biological small molecules [12], and biological imaging [13] due to their strong luminescence intensity, good photo-stability, controllable size, adjustable emission wavelength, and good biocompatibility. For probe assembly, over the years, researchers have utilized peptides, polymers, and proteins as stabilizers to prepare Au NCs [14, 15]. Some proteins can be used as both reductants and stabilizers so that the synthesis does not require additional reductants. The protein scaffolds commonly used for Au NCs include lysozyme [16], horseradish peroxidase [17], deoxyribonuclease [18], and bovine serum albumin (BSA) [19]. These protein scaffolds still retain their inherent biological properties, which means that the Au NC has good biological functionality [20]. BSA is one of the best scaffold proteins to synthesize Au NCs [21]. BSA is readily available, inexpensive, and can act both as a reducing agent and as a stabilizer agent.

✉ Minghui Yang
yangminghui@csu.edu.cn

✉ Avraham Rasooly
rasoolya@mail.nih.gov

[1] Hunan Provincial Key Laboratory of Micro & Nano Materials Interface Science, College of Chemistry and Chemical Engineering, Central South University, Changsha 410083, China

[2] National Cancer Institute, National Institutes of Health, Rockville, MD 20850, USA

In addition to metal nanoclusters, lanthanide(III) elements have interesting photoluminescence properties, such as large Stokes shift and line-like emission spectra with clearly defined bands [22]. Eu^{3+} can be combined with many sites on BSA scaffold, forming strong coordination compounds [23]. Lanthanide(III) ions can be considered as Lewis acid and has a strong tendency to combine with negative charges, neutral oxygen, or nitrogen atoms [24]. These chemical properties enabled the synthesis of different lanthanide(III) complexes for a wide range of bio-detection applications. For example, silicon nanoparticles (SiNPs) modified with Eu(III) were shown to be a viable ratiometric fluorescent probe for tetracycline antibiotics [25]. Calcein-Eu^{3+} was used as recognition group for ATP detection [26]. Iridium(III) was used for temperature sensing in living cells and zebrafish [27].

Eu^{3+} ion has a good response for detecting dipicolinic acid (DPA) [28, 29], a major component of *Bacillus* spores. DPA can be used as a biomarker for *Bacillus anthracis* [30], a major biosafety threat and a safety concern for the food and medical product industry. Due to high resistance to heat, radiation, and chemical processing [31], conventional sterilization technologies cannot normally kill *Bacillus* spores. The resistance of the spores is mainly the result of the highly dehydrated state of the core and the high density of calcium pyridicarboxylate. However, once the spores germinate, the resistance will be greatly reduced. Spore germination is mainly divided into two stages: The first stage is that DPA and some cations in the spore core are released, and the core hydrates partially and loses some resistance. The second stage is the further hydration and expansion of the core, resulting in almost total loss of spore resistance and complete spore germination [31]. Accordingly, the level of DPA can reflect the germination process of spores and so as often used as a biomarker for monitoring spore germination [30]. Many studies have explored DPA levels during spore germination, but most of them are disturbed by the complex environment in which spores are located. Accurate and sensitive detection of DPA as a biomarker for spore presence, germination, and viability can provide an alternative to the time-consuming and tedious direct characterization of intact bacterial cells or the traditional in vivo plate-counting methods [32]. A ratiometric probe for DPA with internal reference may simplify and improve *Bacillus* spore testing. Considering the advantageous properties of Au NCs and lanthanides as fluorescent fluorophores, we synthesized Eu^{3+}-doped Au NC ratiometric probe for detecting DPA. Compared to other fluorescence probes [33], the dual-channel fluorescent probe in this work was synthesized by a one-step method, which not only has good water solubility and luminescence stability, but also realized DPA ratio detection with a low detection limit in complex systems.

Experimental section

Materials and reagents $EuCl_3 \cdot 3H_2O$, dodecylamine, dipicolinic acid, benzoic acid, 2-dipicolinic acid, benzoic acid, terephthalic acid, isophthalic acid, and chloroauric acid ($HAuCl_4 \cdot 3H_2O$) were obtained from Sigma-Aldrich (https://www.sigmaaldrich.com). Bovine serum albumin (BSA) was provided by Sangon Biotech Co., Ltd. (Shanghai, China, https://www.sangon.com/). *Bacillus subtilis* (reference ID ATCC6633) was obtained from Shanghai Luwei Technology Co. Ltd. (Shanghai, China). All other reagents were of analytical grade and used without further purification. Ultrapure water was used throughout all experiments.

Apparatus The fluorescence spectra and relative fluorescence intensity were measured on an F-7000 spectrofluorometer (Hitachi, Japan) with a fixed excitation of 530 nm. Absorption spectra were recorded on a Shimadzu UV-2450 spectrophotometer. Transmission electron microscope (TEM) characterization was performed on an FEI Titan G2 60-300 microscopy. X-ray photoelectron spectroscopy (XPS) investigation was carried out in a Thermo ESCALAB 250Xi using a Al Kα X-ray source (150 W, Mono 500 μm).

Synthesis of Eu^{3+}-Au NC probe The fluorescence probe was prepared by a one-pot method. In brief, 1 mL of $HAuCl_4$ solution (5 mM) and 1 mL of $EuCl_3 \cdot 3H_2O$ solution (5 mM) were quickly mixed with 1 mL of BSA solution (50 mg mL^{-1}) with vigorous stirring. After 5 min, 100 μL of sodium hydroxide solution (1 M) was added dropwise into the mixture. Afterward, the mixture was stirred constantly for 12 h at 37 °C. The solution was centrifuged at 13000 rpm for 30 min, and the supernatant was transferred to a dialysis bag (14 kDa) for 24 h to remove excess impurities. The Eu^{3+}-Au NC probe was stored at 4 °C for further use.

Fluorescent determination of DPA To utilize Eu^{3+}-Au NC probe for DPA determination, 20 μL of the Eu^{3+}-Au NC solution was added into 480 μL solution with various concentrations of DPA. The mixture solution was then incubated for 10 min at room temperature before fluorescence analysis. Fluorescence emission spectra were recorded when excited at 530 nm.

Preparation of the *Bacillus subtilis* spore suspension The spore suspension was prepared as follows: The third culturing generation of *Bacillus subtilis* strains was cultured on the inclined surface of the test tube in unfavorable environmental conditions without nutrients at 37 °C for 1 week to sporulate. After this incubation, the spores on the slope were slightly collected into a centrifuge tube and washed twice with distilled water. The spores were then centrifuged at 5000*g* for 10 min at 4 °C and re-suspended in sterilized water. It was stored at 4 °C for further use.

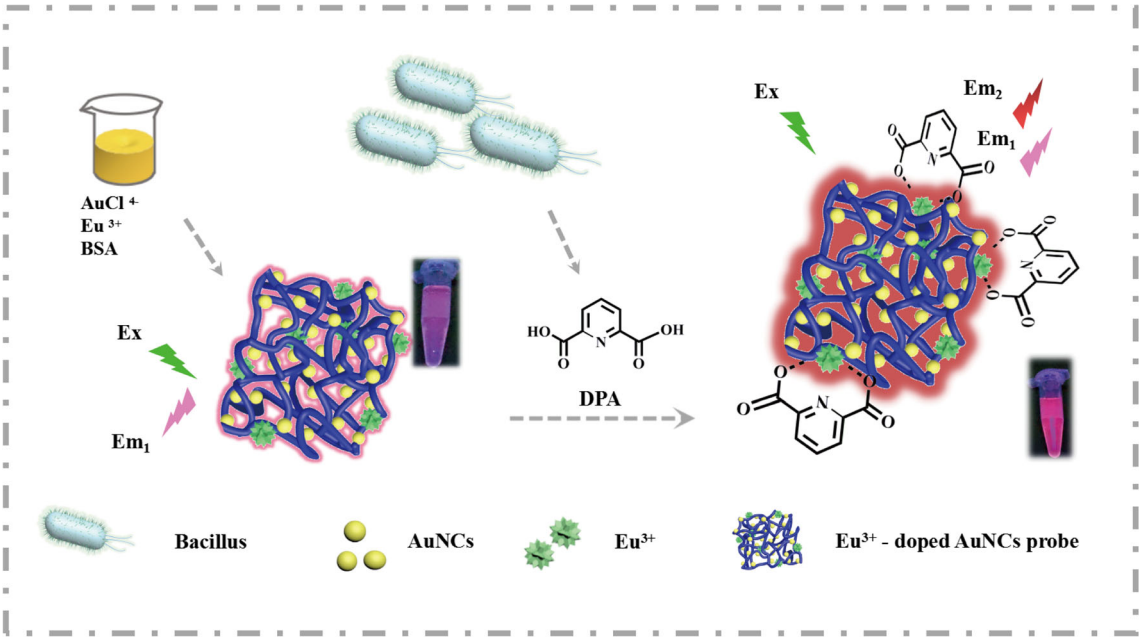

Scheme 1 Schematic diagram of the fluorescent probe preparation and detection process

Detection of the DPA in spores The spore suspension (6.23×10^9 CFU mL^{-1}) was diluted stepwise to lower concentrations (4.0×10^4–6.23×10^6 CFU mL^{-1}). Then, 1 mL of dodecylamine (20 mM) was added to 9 mL of solution with different concentrations of spores and heated for 30 min at 90 °C. The mixture was then centrifuged, and the supernatant was carefully collected. After that, 480 μL of supernatant was mixed with 20 μL of the Eu^{3+}-Au NC probe solution. The

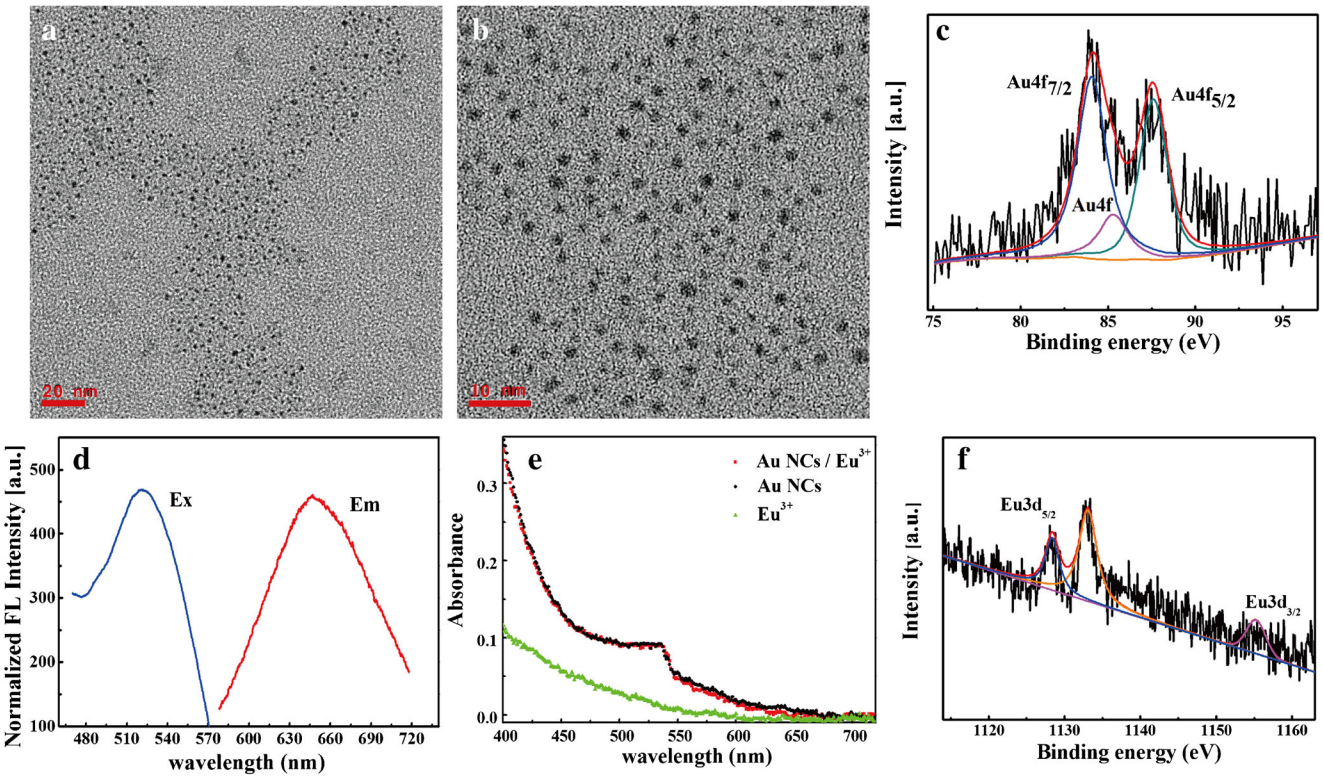

Fig. 1 **a** and **b** TEM images of the synthesized Eu^{3+}-Au NC probe. **c** XPS survey of the Eu 3*d* spectra for Eu^{3+}-Au NC probe. **d** Fluorescence excitation and emission spectra of the Eu^{3+}-Au NC probe. **e** UV-vis absorption of Au NCs, Eu^{3+}-Au NC probe, and Eu^{3+}-BSA complex. **f** XPS survey of the Au 4*f* spectra for Eu^{3+}-Au NC probe

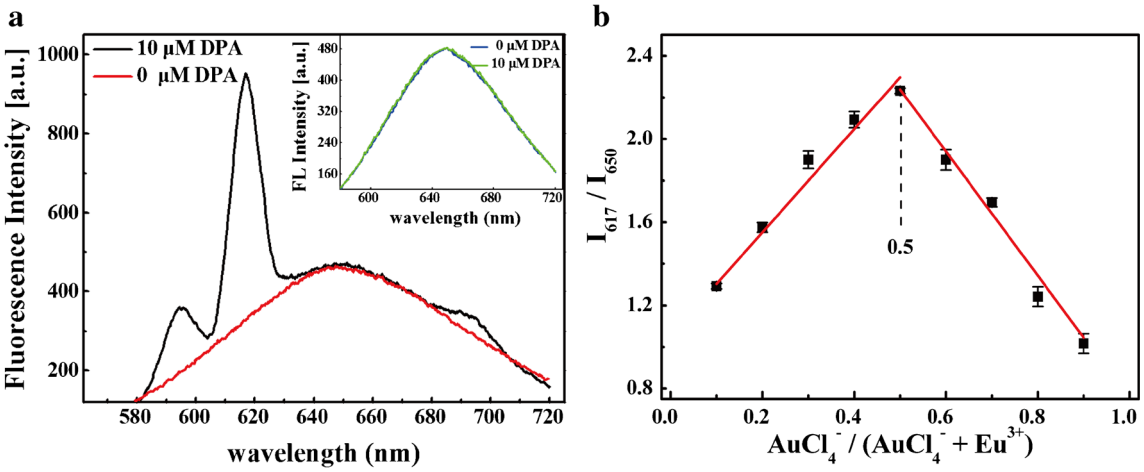

Fig. 2 **a** Fluorescence response of Eu^{3+}-Au NC probe and Au NCs (inset) to 10 μM of DPA. **b** Job's plot for determination of stoichiometry between $AuCl_4^-$ and Eu^{3+}

mixture was incubated for 10 min before the fluorescence emission spectrums were recorded. Colorimetric assay of DPA was performed using ammonium iron(II) sulfate and ascorbic acid according to literature report [34].

Results and discussion

Preparation and characterization of the fluorescence probe

The new ratiometric fluorescence probe utilizes Au NCs as the fluorophore reference and Eu^{3+} ion as a response signal for sensitive determination of DPA. We synthesized the Eu^{3+}-doped Au NC fluorescent probe through a one-pot process. The probe was synthesized by simply adjusting the pH of the mixture containing BSA, Eu^{3+}, and $AuCl_4^{-1}$. BSA plays multiple and critical roles in the design of the probe. BSA serve as scaffold for synthesis to assemble the Eu^{3+} and $[AuCl_4]^-$ utilizing the carboxyl groups and thiol groups to form BSA-Eu and BSA-Au complexes [23]. The formation of Au NCs was initiated by adding NaOH (1 M) into the above solution. The amino acid residues of BSA can reduce Au(III) to gold atoms, and the thiol groups of BSA can form Au-S bonds with Au NCs, making the synthesized Au NCs remarkably stable. Due to the addition of DPA that will not change the structure of Au NCs or chelate it, the fluorescence intensity which belongs to Au NCs will not be affected, and the emission intensity of Au NCs can be used as an internal fluorescence reference to eliminate background interference. The fluorescence of Eu^{3+} signal is significantly enhanced in the presence of DPA due to stable coordination between Eu^{3+} and DPA [35, 36]. The f-f transition between 4*f* layers involved in rare earth is transition resistant, resulting in low luminescence efficiency of rare earth ions. Organic carboxylic acid ligands have high ultraviolet light absorption coefficient. If the triple-excited level and excited-state energy level match with rare earth ions, it can effectively transfer the excited state energy to the emission of rare earth ions, thus sensitizing luminescence of rare earth ions. The luminescence of complexes depends largely on the intramolecular energy transfer efficiency between ligands and rare earth ions [37, 38]. Therefore, Eu^{3+} is used as a signal molecule with a linear response to the concentration of DPA. Scheme 1 illustrates the detection process of DPA using the probe.

Table 1 Comparison for the designed work and other DPA detection methods

Composition of probe	Limit of detection	Linear range	Reference
SiQDs-NH_2-EDTA-Eu	1.02 μM	1.02–34 μM	[6]
Eu/HAP-NPs	0.077 μM	0.1–40 μM	[28]
Eriochrome Black T/Eu^{3+}	2 μM	2–32 μM	[29]
Metal-organic frameworks	4.5 μM	4.5–80 μM	[43]
Naphthalimide/DNA	0.012 μM	0.012–9 μM	[44]
Tb/SiO_2-Eu/GMP	0.05 μM	0.05–2 μM	[45]
Eu^{3+}-Au NCs	0.8 μM	1–50 μM	This work

The TEM image (Fig. 1 a and b) shows the synthesized Au NCs are homogeneous with an average diameter of around 1 nm. XPS was applied to demonstrate the chemical state of the Au and Eu in the Eu^{3+}-Au NC probe (Fig. 1 c). Two characteristic peaks at 84.0 eV for Au $4f_{7/2}$ and 87.7 eV for Au $4f_{5/2}$ are observed [39]. The binding energies at 1126.4 eV and 1154.9 eV correspond to the Eu $3d_{5/2}$ and Eu $3d_{3/2}$ spin-orbit peaks of Eu^{3+} respectively (Fig. 1 f), which suggest the successful synthesis of Eu^{3+}-Au NC fluorescent probe [40]. UV-vis absorption spectra show that Eu^{3+} has no absorption peaks, while the formed Au NCs show an absorption peak at 530 nm (Fig. 1 e). Further characterization of the probe by fluorescence spectrometry shows that the probe displays a

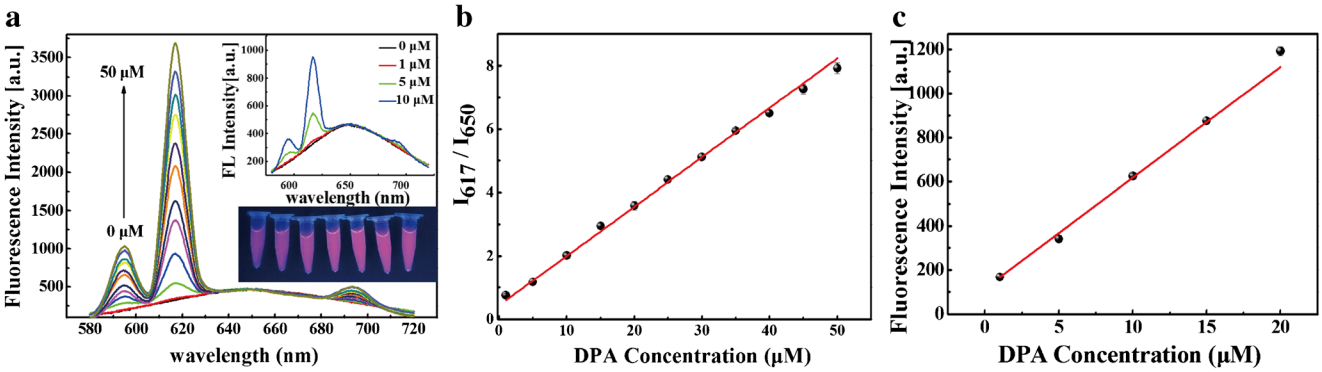

Fig. 3 **a** Responses of the ratiometric probe to different concentrations of DPA, the inset shows the enlarged graph for determination of DPA from 0 to 10 μM and the picture of the fluorescent probes under UV light at different DPA concentrations from 0 to 50 μM. **b** The linear calibration plot of the ratiometric assay to DPA. The fluorescence intensity ratio (I_{617}/I_{650}) was recorded to draw the calibration plot. **c** The linear calibration plot to DPA based on probe with solely Eu^{3+} without Au NCs

broad and relatively weak emission at 650 nm with excitation wavelength of 530 nm (Fig. 1d). This fluorescence emission peak is ascribed to Au NCs [41], which suggests that in the absence of DPA, Eu^{3+} has no fluorescence emission. The fluorescence of Eu^{3+} cannot be detected at this stage probably because of the low amount of Eu^{3+} in the probe. The luminescence quantum yield (QY) of Au NCs was 3.6% using Rhodamine B as the standard in water [42]. Nevertheless, with the introduction of 10 μM of DPA, on the broad emission spectra of Au NCs, two strong and narrow new emission peaks appeared at 595 nm and 617 nm along with another rather weak emission at 695 nm (Fig. 2 a). The fluorescence intensity at 617 nm is about 2.5 times that of 595 nm. The new emission peaks are due to the reaction of DPA with Eu^{3+} ions that enhanced the fluorescence intensity of Eu^{3+} ions. What is more worth mentioning is that the emission intensity of Au NCs at 650 nm does not change, probably because Au NC does not react with DPA, suggesting that the Au NC is a good internal reference probe for DPA detection. These data demonstrated that the synthesized ratiometric fluorescence probe is effective for accurate detection of DPA. In the following experiments, the fluorescence intensity ratio at 617 nm to 650 nm (I_{617}/I_{650}) was used for the analysis of different concentrations of DPA.

Optimization of DPA determination During the probe synthesis process, we observed that by changing the ratio of $AuCl_4^{-1}$ to Eu^{3+}, the color of the synthesized probe would gradually change from clear to light yellow, and finally to white suspension with almost no fluorescence emission. We optimized the ratio of $AuCl_4^{-1}$ to Eu^{3+} for the synthesis of the probe and the optimal ratio is determined to be 1:1 based on the fluorescence Job's plot (Fig. 2 b). At this ratio, for the determination of 10 μM of DPA, I_{617}/I_{650} reached the highest value which is the highest sensitivity of the assay. Besides, the incubation time of the probe with DPA was optimized. The results showed that mixing the probe with DPA produced strong fluorescence emission signal immediately at 617 nm (Figure S1 and S2).

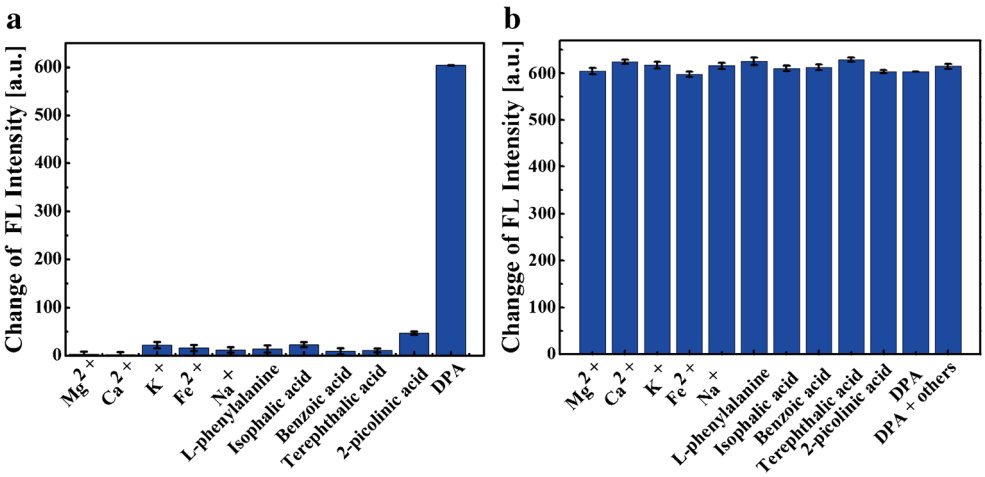

Fig. 4 **a** Responses of the ratiometric probe to 10 μM of DPA and 100 μM of different interfering substances. **b** Responses of the ratiometric probe to 10 μM of DPA and the mixture of 10 μM of DPA with 100 μM of different interfering substances. Others in the figure mean the mixture of all the interfering substances

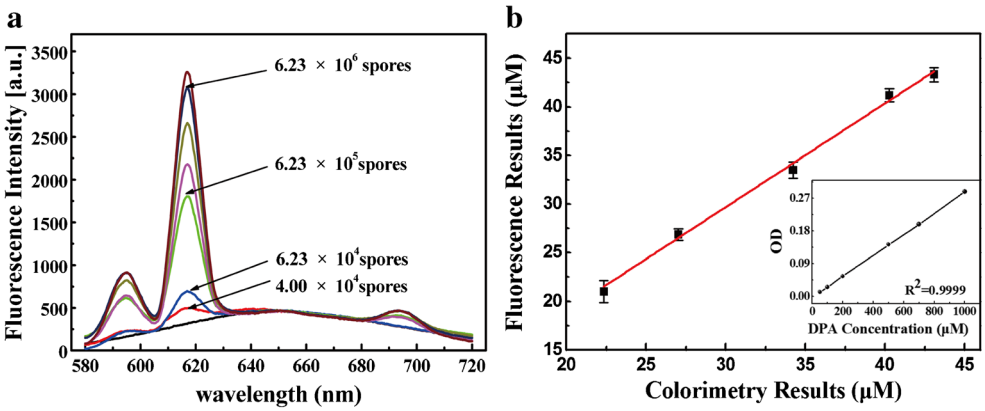

Fig. 5 **a** Response of the probe to DPA released from various concentrations of germinated spores. **b** Correlation of DPA level released from spores determined by the ratiometric probe vs. the level detected by colorimetric method. The inset is the linear range of the colorimetric assay to DPA

Performance of the probe for DPA determination After demonstrating fluorescence characteristics of the probe, the probe was used for ratiometric measurements of DPA. To measure the linear determination range of the probe for DPA, various concentrations of DPA in the range of 0–100 μM were incubated with the probe for 10 min at room temperature, followed by emission spectra measurements. As shown in Fig. 3a, with the increasing concentration of DPA, the fluorescence intensity at 595 nm, 617 nm, and 695 nm are all increased, especially the fluorescence intensity at 617 nm, while there is no fluorescence intensity variation at the 650 nm reference channel (Fig. 3a). With dual-channel ratiometric measurements, a good linear relationship exists between DPA concentration of 1–50 μM and fluorescence intensity ratio (I_{617}/I_{650}) compared with the range of 1–20 μM for the determination with the only Eu^3, without Au NCs (Fig. 3b, c), suggesting that ratiometric approach improves the linear detection range. The detection limits of the ratiometric measurements were calculated to as low as 0.8 μM based on signal to noise ratio of 3. Our data suggest that the Eu^{3+}-Au NC ratiometric fluorescence probe enables detection of DPA with high sensitivity which may enable self-calibration with the control channel measurement. Compared with previously reported luminescence methods, the assay based on Eu^{3+}-Au NCs exhibited a relatively low detection limit as well as a wide linear range (Table 1).

Specificity of fluorescent probe to DPA High probe specificity to the target analyte is essential for sample analysis. To study the specificity of the probe towards DPA, 100 μM of various metal ions and aromatic compounds with similar structures to DPA were tested by the probe. As shown in Fig. 4, the fluorescence responses of compounds used are negligible compared to the determination of 10 μM of DPA (Fig. 4a). Even when these compounds are mixed with DPA, the fluorescence intensity of the mixture does not change much compared to that of DPA alone (Fig. 4b). These results suggest that the probe has high specificity for DPA.

Detection DPA in germinated spores After we demonstrated that the fluorescence probe has good performance for detecting DPA, the probe was applied for the analysis of spore germination. During spore germination, DPA is released from the bacterial spores. Since only after more than two generations of culturing the cells can sporulate effectively, the third generation of *Bacillus subtilis* culture was placed in unfavorable environmental conditions without nutrients for 1 week to induce sporulation and then diluted by 10^9 orders of magnitude for subsequent measurements. The spore germination was induced by adding 2 mM of dodecylamine and the culture was heated at 90 °C for half an hour [31].

As shown in Fig. 5a, with the increase of spore number, the fluorescence signal increased accordingly, with the lowest detection limit of 4×10^4 CFU mL^{-1}. Since the spores themselves do not affect the fluorescence intensity, the increase of fluorescence intensity is attributed to DPA molecules released from the spores. Control experiments of spores that were not treated with dodecylamine showed a very weak fluorescence signal, indicating that non-germinated spores produce little amount of DPA. The production of DPA by the germinated spores was further confirmed by the traditional colorimetric assay. Colorimetric reagent prepared using ammonium iron(II) sulfate and ascorbic acid was used to detect DPA [34]. As shown in Fig. 5b, the amount of DPA produced by the germinated spores detected by our fluorescence probe was highly correlated with those detected by the typical colorimetric method with a correlation coefficient of 0.994 (Fig. 5b).

Traditional methods for spore viability and quantification are based mainly on time-consuming and tedious plate-counting method. Our data demonstrate that the Au NC-based probe can accurately measure the amount of DPA, suggesting that with proper calibration standards, the new probe can be used to accurately measure the level of spore's contamination for food and medical product safety analysis.

Conclusions

We demonstrated here a method for one-step synthesis of Eu^{3+}-doped Au NC fluorescence probe using BSA as scaffold. We have also shown that the probe can be used as a ratiometric fluorescent probe for DPA enabling a low detection limit of 0.8 μM with a linear range of 1–50 μM. The probe design method can be easily adapted to the synthesis of other ratiometric fluorescence probes by altering the doped fluorophores, for example, by using other lanthanide(III) ions, and finding wide applications in various sensing and imaging areas.

Supplementary Information The online version contains supplementary material available at https://doi.org/10.1007/s00604-020-04667-z.

Funding The authors received support of this work from the Hunan Provincial Science and Technology Plan Project, China (No. 2019TP1001) and Innovation-Driven Project of Central South University (2020CX002).

Compliance with ethical standards

Conflict of interest The authors declare that they have no conflict of interest.

References

1. Yao M, Huang J, Deng Z, Jin W, Yuan Y, Nie J, Wang H, Du F, Zhang Y (2020) Transforming glucose into fluorescent graphene quantum dots via microwave radiation for sensitive detection of Al^{3+} ions based on aggregation-induced enhanced emission. Analyst 145:6981–6986
2. Zhang K, Zeng K, Shen C, Tian S, Yang M (2018) Determination of protein kinase A activity and inhibition by using hydroxyapatite nanoparticles as a fluorescent probe. Microchim Acta 185(4):225
3. Li Y, Shen C, Li X, Yang M, Shao C (2018) Hydroxyapatite nanoparticle based fluorometric determination and imaging of cysteine and homocysteine in living cells. Microchim Acta 185(5):271
4. Yang Z-R, Wang M-M, Wang X-S, Yin X-B (2017) Boric-acid-functional lanthanide metal–organic frameworks for selective ratiometric fluorescence detection of fluoride ions. Anal Chem 89(3):1930–1936
5. Edwardson TG, Mori T, Hilvert D (2018) Rational engineering of a designed protein cage for siRNA delivery. J Am Chem Soc 140(33):10439–10442
6. Liu Z, Jin W, Wang F, Li T, Nie J, Xiao W, Zhang Q, Zhang Y (2019) Ratiometric fluorescent sensing of Pb^{2+} and Hg^{2+} with two types of carbon dot nanohybrids synthesized from the same biomass. Sensor Actuator B Chem 296:126698
7. Lee KL, Murray AA, Le DH, Sheen MR, Shukla S, Commandeur U, Fiering S, Steinmetz NF (2017) Combination of plant virus nanoparticle-based in situ vaccination with chemotherapy potentiates antitumor response. Nano Lett 17(7):4019–4028
8. Ganganboina AB, Dutta Chowdhury A, R-a D (2018) N-doped graphene quantum dots-decorated V2O5 nanosheet for fluorescence turn off–on detection of cysteine. ACS Appl Mater Interfaces 10(1):614–624
9. Zhao J, Gao J, Xue W, Di Z, Xing H, Lu Y, Li L (2018) Upconversion luminescence-activated DNA nanodevice for ATP sensing in living cells. J Am Chem Soc 140(2):578–581
10. Zhu S, Zhuo Y, Miao H, Zhong D, Yang X (2015) Detection of mercury (II) by DNA templated gold nanoclusters based on forming thymidine–Hg2+−thymidine duplexes. Luminescence 30(5):631–636
11. Ding S-N, Li C-M, Gao B-H, Kargbo O, Wan N, Chen X, Zhou C (2014) Probing phosphate ion via the europium (III)-modulated fluorescence of gold nanoclusters. Microchim Acta 181(15–16): 1957–1963
12. Feng L-P, Yang J-N, Zhang S, Zhang L-X, Chen X, Li P, Gao Y, Xie S-J, Zhang Y, Wang H (2020) A capillary-based fluorimetric platform for the evaluation of glucose in blood using gold nanoclusters and glucose oxidase in the ZIF-8 matrix. Analyst 145(15):5273–5279
13. Cruz-Alonso M, Fernandez B, García M, Hc G-I, Pereiro R (2018) Quantitative imaging of specific proteins in the human retina by laser ablation ICPMS using bioconjugated metal nanoclusters as labels. Anal Chem 90(20):12145–12151
14. Yamamoto H, Yano H, Kouchi H, Obora Y, Arakawa R, Kawasaki H (2012) N, N-Dimethylformamide-stabilized gold nanoclusters as a catalyst for the reduction of 4-nitrophenol. Nanoscale 4(14): 4148–4154
15. Liang R, Xie J, Li J, Wang K, Liu L, Gao Y, Hussain M, Shen G, Zhu J, Tao J (2017) Liposomes-coated gold nanocages with antigens and adjuvants targeted delivery to dendritic cells for enhancing antitumor immune response. Biomaterials 149:41–50
16. Chen TH, Tseng WL (2012) (Lysozyme type VI)-stabilized Au_8 clusters: synthesis mechanism and application for sensing of glutathione in a single drop of blood. Small 8(12):1912–1919
17. Zhuo Y, Yi W-J, Lian W-B, Yuan R, Chai Y-Q, Chen A, Hu C-M (2011) Ultrasensitive electrochemical strategy for NT-proBNP detection with gold nanochains and horseradish peroxidase complex amplification. Biosens Bioelectron 26(5):2188–2193
18. Li Z-Y, Wu Y-T, Tseng W-L (2015) UV-light-induced improvement of fluorescence quantum yield of DNA-templated gold nanoclusters: application to ratiometric fluorescent sensing of nucleic acids. ACS Appl Mater Interfaces 7(42):23708–23716
19. Ju YJ, Li N, Liu SG, Han L, Xiao N, Luo HQ, Li NB (2018) Ratiometric fluorescence method for malachite green detection based on dual-emission BSA-protected gold nanoclusters. Sensors Actuators B Chem 275:244–250
20. West AL, Griep MH, Cole DP, Karna SP (2014) DNase 1 retains endodeoxyribonuclease activity following gold nanocluster synthesis. Anal Chem 86(15):7377–7382
21. Sheng J, Jiang X, Wang L, Yang M, Liu Y-N (2018) Biomimetic mineralization guided one-pot preparation of gold clusters anchored two-dimensional MnO2 nanosheets for fluorometric/magnetic bimodal sensing. Anal Chem 90(4):2926–2932
22. Liu B, Shen H, Hao Y, Zhu X, Li S, Huang Y, Qu P, Xu M (2018) Lanthanide functionalized metal–organic coordination polymer: toward novel turn-on fluorescent sensing of amyloid β-peptide. Anal Chem 90(21):12449–12455
23. Kort R, O'brien AC, Van Stokkum IH, Oomes SJ, Crielaard W, Hellingwerf KJ, Brul S (2005) Assessment of heat resistance of bacterial spores from food product isolates by fluorescence monitoring of dipicolinic acid release. Appl Environ Microbiol 71(7): 3556–3564
24. Binnemans K (2009) Lanthanide-based luminescent hybrid materials. Chem Rev 109(9):4283–4374
25. Lin B, Zhang T, Xin X, Wu D, Huang Y, Liu Y, Cao Y, Guo M, Yu Y (2019) Europium (III) modified silicone nanoparticles for ultrasensitive visual determination of tetracyclines by employing a fluorescence color switch. Microchim Acta 186(7):442

26. Zhang C, Zhang H, Yu Y, Wu S, Chen F (2019) Ratio fluorometric determination of ATP base on the reversion of fluorescence of calcein quenched by Eu (III) ion using carbon dots as reference. Talanta 197:451–456
27. Zhang H, Jiang J, Gao P, Yang T, Zhang KY, Chen Z, Liu S, Huang W, Zhao Q (2018) Dual-emissive phosphorescent polymer probe for accurate temperature sensing in living cells and zebrafish using ratiometric and phosphorescence lifetime imaging microscopy. ACS Appl Mater Interfaces 10(21):17542–17550
28. Li Y, Li X, Wang D, Shen C, Yang M (2018) Hydroxyapatite nanoparticle based fluorometric turn-on determination of dipicolinic acid, a biomarker of bacterial spores. Microchim Acta 185(9):435
29. Yilmaz MD, Oktem HA (2018) Eriochrome black T–Eu3+ complex as a ratiometric colorimetric and fluorescent probe for the detection of dipicolinic acid, a biomarker of bacterial spores. Anal Chem 90(6):4221–4225
30. Liang X-S, Liu C, Long Z, Guo X-H (2018) Rapid and simple detection of endospore counts in probiotic Bacillus cultures using dipicolinic acid (DPA) as a marker. AMB Express 8(1):101
31. Setlow P (2006) Spores of Bacillus subtilis: their resistance to and killing by radiation, heat and chemicals. J Appl Microbiol 101(3): 514–525
32. Hazan R, Que Y-A, Maura D, Rahme LG (2012) A method for high throughput determination of viable bacteria cell counts in 96-well plates. BMC Microbiol 12(1):1–7
33. Wang J, Li D, Qiu Y, Liu X, Huang L, Wen H, Hu J (2020) An europium functionalized carbon dot-based fluorescence test paper for visual and quantitative point-of-care testing of anthrax biomarker. Talanta 220:121377
34. Shah IM, Laaberki M-H, Popham DL, Dworkin J (2008) A eukaryotic-like Ser/Thr kinase signals bacteria to exit dormancy in response to peptidoglycan fragments. Cell 135(3):486–496
35. Wang J, de Kool RM, Velders AH (2015) Lanthanide-dipicolinic acid coordination driven micelles with enhanced stability and tunable function. Langmuir 31(44):12251–12259
36. Singhal P, Vats BG, Jha SK, Neogy S (2017) Green, water-dispersible photoluminescent on–off–on probe for selective detection of fluoride ions. ACS Appl Mater Interfaces 9(24):20536–20544
37. Choppin GR, Peterman DR (1998) Applications of lanthanide luminescence spectroscopy to solution studies of coordination chemistry. Coord Chem Rev 174(1):283–299
38. Song J-F, Jia Y-Y, Zhou R-S, Li S-Z, Qiu X-M, Liu J (2017) Six new coordination compounds based on rigid 5-(3-carboxy-phenyl)-pyridine-2-carboxylic acid: synthesis, structural variations and properties. RSC Adv 7(12):7217–7226
39. Magde D, Rojas GE, Seybold PG (1999) Solvent dependence of the fluorescence lifetimes of xanthene dyes. Photochem Photobiol 70(5):737–744
40. Zhou Q, Lin Y, Xu M, Gao Z, Yang H, Tang D (2016) Facile synthesis of enhanced fluorescent gold–silver bimetallic nanocluster and its application for highly sensitive detection of inorganic pyrophosphatase activity. Anal Chem 88(17):8886–8892
41. Yu Y, Yang Y, Ding J, Meng S, Li C, Yin X (2018) Design of a biocompatible and ratiometric fluorescent probe for the capture, detection, release, and reculture of rare number CTCs. Anal Chem 90(22):13290–13298
42. Jia J, Zhang Y, Zheng M, Shan C, Yan H, Wu W, Gao X, Cheng B, Liu W, Tang Y (2018) Functionalized Eu (III)-based nanoscale metal–organic framework to achieve near-IR-triggered and-targeted two-photon absorption photodynamic therapy. Inorg Chem 57(1):300–310
43. Shi K, Yang Z, Dong L, Yu B (2018) Dual channel detection for anthrax biomarker dipicolinic acid: the combination of an emission turn on probe and luminescent metal-organic frameworks. Sensors Actuators B Chem 266:263–269
44. Wang Q-X, Xue S-F, Chen Z-H, Ma S-H, Zhang S, Shi G, Zhang M (2017) Dual lanthanide-doped complexes: the development of a time-resolved ratiometric fluorescent probe for anthrax biomarker and a paper-based visual sensor. Biosens Bioelectron 94:388–393
45. Verma M, Kaur N, Singh N (2018) Naphthalimide-based DNA-coupled hybrid assembly for sensing Dipicolinic acid: a biomarker for Bacillus anthracis spores. Langmuir 34(22):6591–6600